01 Aug 2002

Surface Switching Characteristics of Variable Permittivity Dielectrics

Wayne Huebner
Missouri University of Science and Technology, huebner@mst.edu

Eric J. Carleton

Recommended Citation

W. Huebner and E. J. Carleton, "Surface Switching Characteristics of Variable Permittivity Dielectrics," *IEEE Transactions on Dielectrics and Electrical Insulation*, vol. 9, no. 2, pp. 253-262, Institute of Electrical and Electronics Engineers (IEEE), Aug 2002.
The definitive version is available at https://doi.org/10.1109/94.993743

Surface Switching Characteristics of Variable Permittivity Dielectrics

Eric J. Carleton and Wayne Huebner
University of Missouri-Rolla
Rolla, MO 65409, USA

ABSTRACT

Flashover voltage, lifetimes, and switch performance of insulators utilizing square thin and thick film electrodes were examined to determine the viability of using thin electrodes for reliable surface discharge switching. Gold, silver, and platinum were sputtered (0.25μm) and screen printed (15μm) onto Al_2O_3, TiO_2, and a modified $BaTiO_3$ (MBT), then tested in air at 10^5 Pa, under vacuum (10^{-3} torr), and while immersed in an insulating fluid, SF-2 (manufactured by 3M). For the measured range of 0.5 to 3mm in air, the flashover voltage for all three insulators was found to have a linear dependence on the electrode separation distance with 15μm thick screen printed electrodes and a square root dependence with 0.25μm thick sputtered electrodes. Delay times of approximately 20ns with a corresponding jitter of 6ns were observed across all three insulators under triggered flashover. Insulators in air with sputtered electrodes had lifetimes of approximately 5 flashovers for dc flashover and 40 for triggered flashover. Screen printed TiO_2 and MBT had dc lifetimes of approximately 10 flashovers in air, and 3 flashovers in vacuum and SF-2. Screen printed TiO_2 and MBT had triggered lifetimes of greater than 200 flashovers in air, and < 3 flashovers in vacuum and SF-2. Screen printed Al_2O_3 had dc and triggered lifetimes of greater than 200 flashovers in air, vacuum and SF-2. Insulator failure during dc flashover was determined to be due to the formation of a conductive channel between the anode and cathode. Formation of the channel was attributed to insulator thermal and dielectric properties and the presence of vaporized electrode species in the gap region during flashover.

1 INTRODUCTION

MUCH research in the literature has focused on flashover voltage models, mechanisms, and behavior in vacuum gaps bridged by insulators. Many surface flashover models in vacuum have been debated and consist of sub-surface and above-surface processes initiating the flashover [1, 2], however recent research efforts support an above-surface model with at least four distinct phases: 1. field emission of electrons from the cathode, 2. field emitted electrons impinge upon the surface of the dielectric, leading to an electron avalanche governed by the secondary electron emission coefficients, 3. build-up of local pressure due to electron stimulated outgassing, and 4. gaseous ionization and breakdown [3, 4]. The primary focus is usually the abatement of such discharges, however in some instances control over the discharge event is desirable. For instance, surface discharge switches are used to switch large amounts of power due to their intrinsic short delay time with minimal jitter [5]. High power surface discharge switches typically consist of large electrodes and insulators with large thermal masses that avoid catastrophic failure through dielectric ablation and thermal conduction away from the discharge site. A few papers have mentioned the use of thin electrodes for studying surface flashover models more thoroughly [6, 7], but to the authors knowledge only limited data are available on switching voltages, waveforms, and lifetimes for thin electrode, high dielectric constant surface switches. These are potentially important for switching asymmetric Blumleins such as in the Dielectric Wall Accelerator (DWA) proposed by Lawrence Livermore National Laboratory (LLNL) [8–10]. Due to design constraints, it is desirable if the thin electrodes sandwiched between the plates can function as surface switches triggered by a laser or electrical impulse [11]. This paper presents a comprehensive summary and explanation of the flashover voltages, lifetimes, and switch performance of thin electrode switches under successive switching in air, vacuum, and insulating fluid with variation in electrode material and deposition method, insulator dielectric constant, and surface roughness and contamination.

2 EXPERIMENTAL PROCEDURE

Al_2O_3, TiO_2, and modified $BaTiO_3$ (MBT) were chosen as insulators for this study based on their order of

1070–9878/1/$17.00 © 2002 IEEE

Table 1. Insulator and electrode material properties [29,30].

	K (unitless)	$\sigma_{thermal}$ (W/m·K)	ΔH_f (kJ/mol)	ϕ_w (eV)	T_m (°C)
Insulator					
MBT	2000	2.9	—	—	1620
TiO_2	100	6.5	−994	—	1850
Al_2O_3	11	30	−1676	—	2100
NaCl	6	6.4	−411	—	800
Quartz	3.8	1.4	—	—	1680
Teflon	2	2.3	−820	—	320
Electrode					
Ag	—	429	—	4.26	962
Au	—	317	—	5.10	1064
Pt	—	72	—	5.65	1772

magnitude of differing dielectric constants as tabulated in Table 1. NaCl, fused quartz, and polytetrafluoroethylene (PTFE) were used in a few experiments due to their low dielectric constant, thermal conductivity, and melting temperature. Silver, gold, and platinum were chosen as electrode materials on the basis of their varying melting temperature and work functions which are also shown in Table I. The electrodes were deposited by both screen printing and sputtering as they are two widely used and affordable electrode deposition methods.

Cylindrical insulators (6 cm in diameter, 1.5 mm thick) of TiO_2 (Aesar 99.9%) and the modified $BaTiO_3$ (TAM 412H) were prepared by conventional sintering techniques and had theoretical densities greater than 95%. Rectangular plates (20 mm long × 15 mm wide × 1.5 mm thick) of Al_2O_3 (Coors Ceramics) were used and had a theoretical density of ≈ 96%. Single crystals of NaCl (SPI-Chem), PTFE sheets, and fused quartz slides were polished to 2 mm in thickness and a surface finish of 5 μm. Two different switch configurations were tested in this study and are illustrated in Figure 1. The electrode gap in configuration I is similar to the proposed LLNL device [8–10], however for ease in testing and fabricating samples, configuration II was used for the majority of the studies. Cylindrical samples of TiO_2 and MBT were vertically sliced to obtain the rectangular cross-section (7 mm wide × 1.5 mm thick) depicted in configuration I. The electrode gap width in configuration II was varied from 0.5 to 3 mm, and the electrode gap in configuration I was set to the thickness of the samples, 1.5 mm. During switching experiments, both configurations were placed directly on top of a nonmetallic insulating table which exposed the top electrode in configuration I and exposed both electrodes in configuration II. The discharge gap was not coincident with the insulating table for either configuration.

The insulator surfaces were polished to a 5 μm surface finish with a SiC slurry. In addition, a few samples were sanded to a surface finishes of 100 and 15 μm to alter the surface roughness so that any physical characteristics might be observed. After polishing, the samples were put in a dilute, agitated nitric acid solution for 8 h. The samples were removed, ultrasonically cleaned in de-ionized water for 0.25 h, and then ultrasonically cleaned in acetone for 0.25 h. Surfaces were examined by a scanning electron microscope (SEM) to verify surface purity. A few samples were not cleaned after polishing so that the effect of the presence of surface contaminants could be observed.

Square (5 mm × 5 mm) Ag electrode pads (Silver Paste Plus, SPI) were screen printed and then heated at 200°C for 0.5 h. to sinter the metal particles, thus resulting in an average thickness of 10 to 15 μm. Sputtered electrode pads of silver, gold, and platinum of the same dimensions were deposited at a rate of 50 nm/min in an argon atmosphere to a final thickness of 0.25 μm. The sputtered electrode samples were then subjected to the same heat treatment schedule to eliminate any thermal conditioning effect associated with gas absorption [12].

dc surface flashover measurements were performed by applying a step-wise bias to the gap in 40 V increments with a high voltage amplifier (Trek 20/20A). Upon insulator flashover, the power supply was manually shut off, and the output voltage was recorded. Discharge voltage and current signals were measured on a digital 2 channel Tektronix 2 Gs/s oscilloscope with a high voltage probe (Tektronix P5100) and a passive ac current probe (Tektronix P6021) with response times of less than 2 and 6 ns respectively. Figure 2 illustrates the measurement setup and circuit used in this study. Measured values were statistically quantified by analyzing 10 samples of each com-

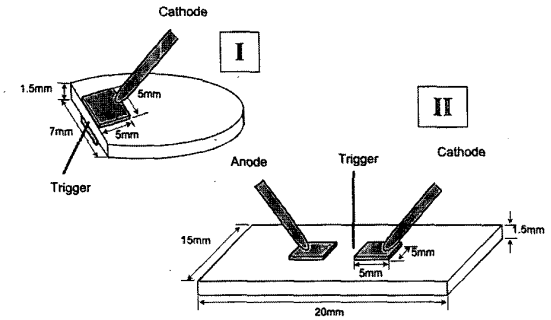

Figure 1. Illustrations of the electrode configurations used in this study.

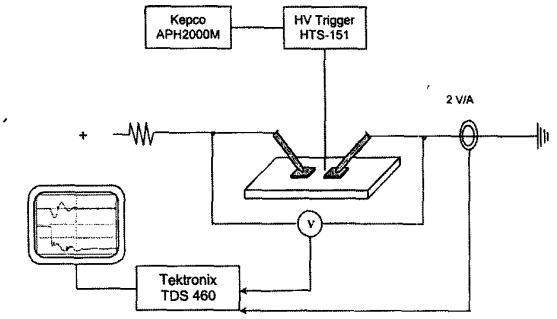

Figure 2. Schematic of the experimental setup for surface flashover.

bination of insulator, gap (0.5, 1, 1.5, 2, 2.5, and 3 mm), and electrode deposition method.

Triggered flashover measurements were taken by applying a variable 0 to +2 kV pulse (20 ns rise, 250 ns width) through a 24 gauge trigger wire centrally positioned 0.25 mm above the surface and 0.25 mm from the cathode [5]. The surface gap was slowly charged to 50% of the DC flashover voltage before the trigger voltage was applied.

Samples were tested at 10^5 Pa, 0.13 Pa (10^{-3} Torr), and while immersed in a non-charring, insulating dielectric liquid SF-2 (manufactured by 3M) to ascertain the viability of device switching in a variety of environments. Atmospheric measurements were conducted in a steady state fashion by placing the sample in a clear plastic container which was sealed upon flushing the container with air passed through drierite to obtain a relative humidity of 35 to 50%.

Before and after breakdown tests, both electrodes and the surface were subjected to microstructural analysis with a scanning electron microscope (Jeol T330A SEM). Carbon coating was used to minimize charging on the insulating surfaces. Chemical analysis of the surface was performed by an energy dispersive spectroscopy (EDS) system attached to the microscope.

During continued dc breakdown, a digital camera (Sony Mavika) was used to capture the discharge trajectory from electrode to electrode. The frame rate of the camera was of the order of 0.01 s, thus time lapsed images of multiple surface discharges were observed.

Electrostatic field modeling was conducted with Integrated Software's Electro 2D v5.1 software to determine field enhancement factors and polarization induced charge contributions at the dielectric/metal/air interface. The software uses the Boundary Element Method to solve for an equivalent source, which would sustain the modeled field under the prescribed boundary conditions determined by the Green's function of the modeled geometry [13, 14].

3 RESULTS AND DISCUSSION

3.1 dc SURFACE FLASHOVER

Typical current and voltage signals detected using single channel dc surface flashover are shown in Figure 3. The oscillatory nature of the current waveform is due to ringing from the short transit time to ground in the measurement circuit. Visually, single channel flashovers appeared to be a single streak traversing the electrode gap. The dc flashover signal exhibited a 20 to 30 ns current rise, subsisted for 100 to 150 ns, and was found to be independent of insulator, atmosphere and electrode deposition method. In the probe detection range, a 5 to 10 ns current rise was expected [4], but the observed rise can be explained by bandwidth limitations of the current probe.

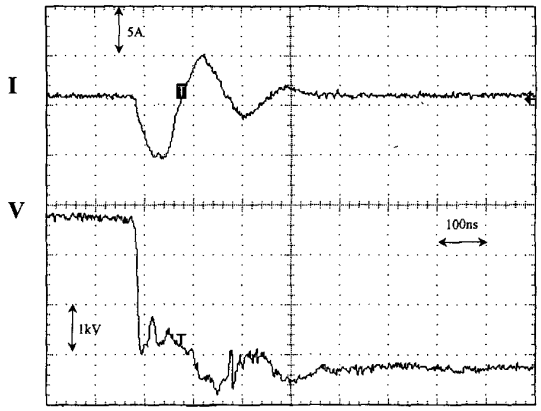

Figure 3. Typical current and voltage signals during a dc flashover.

The voltage across the electrode gap rapidly decreased in 10 ns from the maximum voltage to zero and recovered to the initial flashover voltage after 20 to 30 μs. Previously reported recovery values range from 100 to 300 μs, but those values were for switching much higher currents [15]. The dc recovery voltage exhibited no clear material, voltage, or atmospheric effect and correlates with the recovery time of the high voltage amplifier. The average energy and charge switched per channel varied with the applied switching voltage, but was generally in the range of 0.01 to 0.05 J and 0.3 to 0.5 μC, respectively as determined from integration of the time dependent voltage and current signals.

Multiple channel flashovers were visually observed in the captured digital images as multiple streaks simultaneously traversing the electrode gap. Figure 4 shows typical current and voltage signals detected upon multiple channel surface flashover and indicates that the multiple streaks were not simultaneous. Multiple channel flashovers consisted of individual current and voltage waveforms

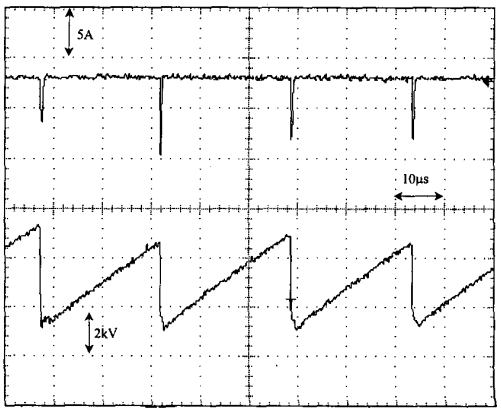

Figure 4. Typical current and voltage signals during consecutive multiple channel dc flashover.

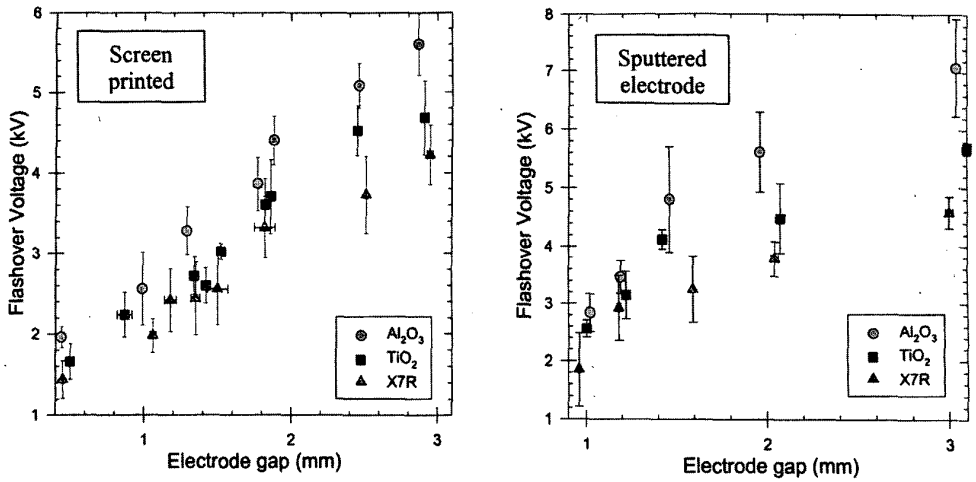

Figure 5. Influence of Ag electrode deposition method on flashover voltage. 15 μm thick screen printed electrodes and 0.25 μm thick sputtered electrodes.

similar to the single channel waveforms, that were separated by 20 to 200 μs between successive waveforms. The presence of multiple streaks in the digital images can be attributed to the relatively long exposure time (10 ms) of the camera. Although both single and multiple channel flashover were electrically observed across all three insulators in air, single channel flashover was predominantly observed across Al_2O_3 and multiple channel flashover was observed across MBT and TiO_2. Flashovers across all three insulators in SF-2 and vacuum were typically multiple channel in nature.

Figure 5 shows the flashover voltage for Al_2O_3, TiO_2, and MBT in air with sputtered and screen printed silver electrodes. For the measured range of 0.5 mm to 3 mm in air, the flashover voltage for all three insulators was found to have a linear dependence on the electrode separation distance with 15 μm thick screen printed electrodes and a square root dependence with 0.25 μm thick sputtered electrodes. A square root dependence is typically experimentally and theoretically observed [5, 16], however studies have also shown linear dependencies with non-zero constants in the 1 to 20 mm separation distance [17, 5]. The difference in thickness and hence mass of the two different electrodes may explain the difference in dependencies. The flashover voltages summarized in Table 2 are the result of 40 samples each and are an average of the observed flashover voltages to failure except for Al_2O_3 with screen printed electrodes, in which the average of the first 30 flashovers is reported. The flashover voltages were found to have a negative relationship with the dielectric constant which agrees with previous studies on high dielectric constant materials [6, 18]. The dc flashover voltages for samples tested at 0.13 Pa and in SF-2 were approximately 300% and 400% higher than the voltages found for samples tested at 1atm. Statistical variation in flashover voltage was not determined because only single flashover lifetimes were observed for the TiO_2 and MBT samples which makes them impractical for use in the DWA.

Although three metals with three different melting temperatures and work functions were sputtered for electrodes, the measured flashover voltages and lifetimes were the same within statistical variation as is shown in Figure 6. Due to the thinness of these electrodes and subsequent small thermal mass (< 3 mg), the melting temperature becomes an insignificant factor in the determination of breakdown characteristics. In addition, the geometry related resistance of the electrodes is of the order 1 Ω which could also contribute to joule heating. The energy transferred in the arc (0.01 to 0.05 J) in the short amount of time could easily lead to melting and vaporization of even most refractory metals with such small thermal mass [19].

The work function of the electrode material was expected to affect the self-breakdown voltages since according to the Fowler-Nordheim theory [20], a metal with a lower work function will emit an appreciable electron current at lower fields than a metal with a higher work function. The enhanced current would then lead to the formation of secondary electron avalanche at lower field values. The lack of observation of this behavior is attributed to the field enhancement created from the high effective radius of curvature of the sputtered electrode and porosity at the metal/dielectric/atmosphere triple point. In a study by Kofoid [6], the relative field enhancement of porosity at the triple point outweighed all other factors in the determination of the flashover voltage.

The flashover voltage dependence on increased surface roughness (5 to 100μm) and the presence of surface contaminants for screen printed electrodes is shown in Figure 6. As shown, no clear flashover dependence can be seen for either surface roughness or removal of surface contaminants from polishing. In previous studies, an increase

Table 2. Flashover voltages of Al_2O_3, TiO_2, MBT studied insulators in air as a function of electrode separation distance, d (mm).

	Screen Printed Electrodes		Sputtered Electrodes	
Insulator	Flashover Voltage (kV)	Error (kV)	Flashover Voltage (kV)	Error (kV)
Al_2O_3	$1.58 \cdot d + 1.17$	± 0.09	$5.66 \cdot d^{1/2} - 2.55$	± 0.29
TiO_2	$1.32 \cdot d + 1.06$	± 0.10	$3.83 \cdot d^{1/2} - 0.99$	± 0.24
MBT	$1.13 \cdot d + 1.03$	± 0.12	$3.29 \cdot d^{1/2} - 1.00$	± 0.21

Table 3. Calculated field enhancement, polarization, and effective surface charge at the dielectric/metal/atmosphere interface.

Insulator	Field Enhancement (unitless)	Polarization ($\mu C/cm^2$)	Effective Charge (μC)
Al_2O_3	7.2	0.12	0.0001
TiO_2	9.4	3.15	0.0017
MBT	10.3	48.00	0.0589

in flashover voltage was observed for materials polished with SiC to a finer finish and for materials subjected to a chemical etch to remove polishing contaminants [21, 22]. An increase in flashover voltage was also noted with a study by Sudarshan and Li [23], however large scatter in the data was also noted. The lack of observation of any flashover trend related to surface contaminants and surface roughness is attributed to the scatter in the collected data which is due to the imperfect edges of the thin electrodes.

A variance in height of the flashover path over the insulator surface in air was also noticed with both screen printed and sputtered electrodes. During flashover across an MBT surface, the path was observed to follow the surface with no visible separation distance between the surface and the flashover. Flashovers across TiO_2 and Al_2O_3 surfaces tended to follow a curved path from electrode to electrode with a maximum separation distance between the surface and flashover of approximately 2 to 3 mm. Neuber, et al [3] observed a curved discharge path across Al_2O_3 in vacuum, 10 min after the initial flashover and attributed this behavior to a lack of replenished gaseous species on the surface of the insulator. In air, however, plenty of gaseous atoms exist near the surface of the insulator, yet the flashover path across Al_2O_3 and TiO_2 still arcs away from the surface.

Electrostatic field modeling was used to calculate the maximum polarization and effective induced charge accumulating at the dielectric/metal/atmosphere triple point due to dielectric constant and field enhancements as summarized in Table 3. The effective charge is integrated across the entire gap region, and the maximum polarization is located within 0.1 mm of the triple point. The increase in polarization for high dielectric constant insulators increases the surface capacitance before flashover, which is known to affect the local field enhancement and propagation speed of the streamers [5]. In such a small gap however, the flashover is predominantly a cathode process involving ionized gas and electrons. The ions and electrons created before flashover also see this increased field and polarization and likewise would be more attracted to the surface thereby creating a flashover path closer to the surface with high dielectric constant materials. Beverly noted a pressing of the flashover plasma across the insulator surface when a ground plane electrode was affixed to the rear of an insulator to increase the surface capacitance of the insulator [24]. The effective polarization and field enhancement calculated at the triple point leads to a lowering of the work function and an increase

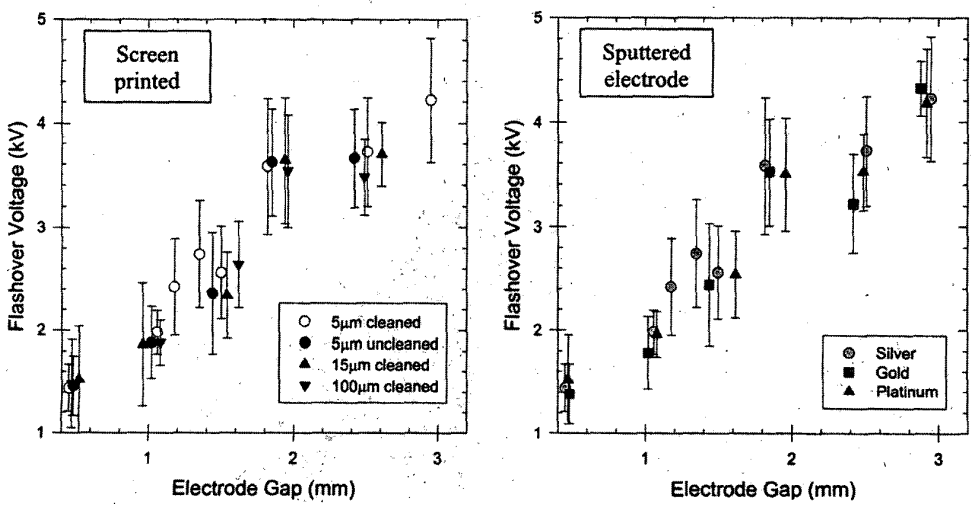

Figure 6. Electrode material, surface finish, and contaminant influence on dc flashover voltage across MBT surface.

Table 4. Observed lifetime values for insulators during dc flashover.

	Screen Printed Electrodes			Sputtered Electrodes		
Insulator	Air	Vacuum	SF2	Air	Vacuum	SF2
Al_2O_3	> 200	> 200	> 200	5.4 ± 2.3	< 3	< 3
TiO_2	4.3 ± 3.1	< 3	< 3	4.4 ± 2.1	< 3	< 3
MBT	2.8 ± 1.7	< 3	< 3	4.4 ± 2.2	< 3	< 3

in the Fowler-Nordheim emission current at lower voltages, which explains the negative trend of flashover voltage with insulator dielectric constant.

A large variance of lifetimes for the samples due to insulator and electrode deposition method was observed. Failure was defined as the point when either the gap was made conductive or when the electrode gap had widened an additional 0.5 mm due to electrode vaporization. A summary of the observed dc surface flashover lifetimes is presented in Table 4. Figure 7 shows a typical sputtered electrode before and after a flashover event. The electrode exhibits a uniform layer over the insulator before flashover, but upon switching, portions of the electrode were vaporized due to joule and ion beam heating [25]. Initiation of successive flashovers were found to require increasingly larger voltages due to a widening of the electrode gap from the vaporization of electrode material as shown in Figure 8. After just a few flashovers, large voltages were required to initiate flashover such that the next flashover removed a bulk of the remaining electrode material due to higher stored energies and led to the failure of the sample. Careful SEM analysis of the electrode gap revealed that negligible amounts of metal were deposited in the electrode gap from the sputtered electrodes. However, random islands of the sputtered electrode film still existed in the initial electrode region as shown in the image in Figure 7.

A typical electrode/insulator image for the screen printed electrodes before and after flashover is shown in Figure 7. Backscattered SEM shows the metallization of the electrode gap from deposited electrode material. The metal hemispheres deposited in the electrode gap were determined by EDS to be composed of the electrode material. The hemispherical shape indicates that the metal was molten upon deposition and became hemispherical due to surface free energy. The edges of the electrode upon flashover were observed to be rounded due to local joule and ion heating, which removed small burrs and protrusions created during screen printing, thereby decreasing local field enhancement factors. This observation might help explain the increase of the flashover voltage upon successive flashovers for screen printed electrodes across Al_2O_3. An increase in the flashover voltage in vacuum has been experimentally shown for an insulator treated with a thin layer of discontinuous metal which could also explain the increase in flashover voltage upon successive flashovers [26].

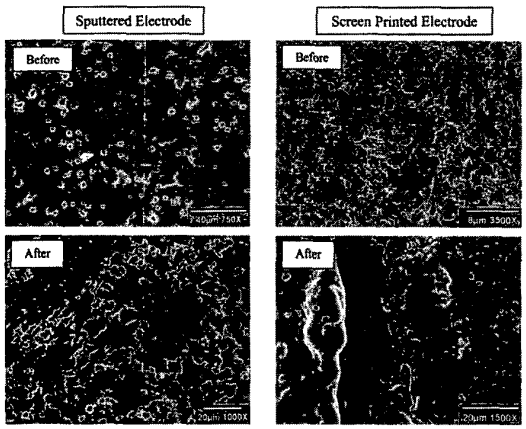

Figure 7. Sputtered and screen printed electrodes before and after flashover experiments depicting the vaporization of the electrode material and subsequent deposition in the gap region.

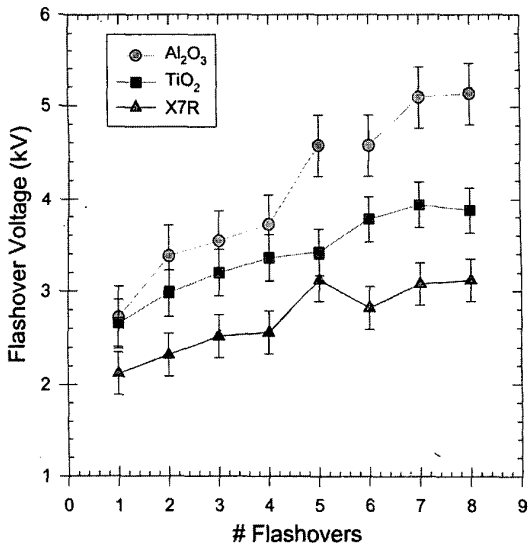

Figure 8. Flashover voltage dependence on the number of flashovers across insulators with sputtered silver electrodes.

As was shown in Table 4, Al_2O_3 exhibited a much larger lifetime with screen printed electrodes in air than did TiO_2 or MBT. Although the Al_2O_3 surface was deposited with electrode material from thousands of flashovers, a continuous, conductive channel was not formed. That was not the case for flashover across TiO_2 and MBT samples however. After a catastrophic flashover, the gap could hold off only 200 to 600V after which the previously formed flashover channel, shown in Figure 9, would carry enough current to radiate due to resistive heating. A dark discharge path is clearly seen to traverse the electrode gap between the anode and cathode. This dark color indicates a lower average atomic number than the surrounding area due to a smaller secondary electron coefficient, and indicates that the black region is TiO_2 and not electrode ma-

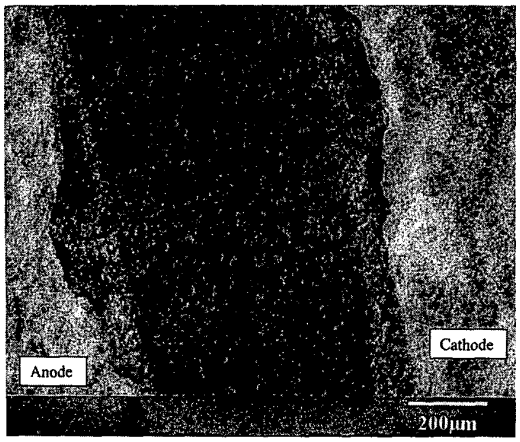

Figure 9. SEM image of a TiO_2 insulator after a catastrophic flashover.

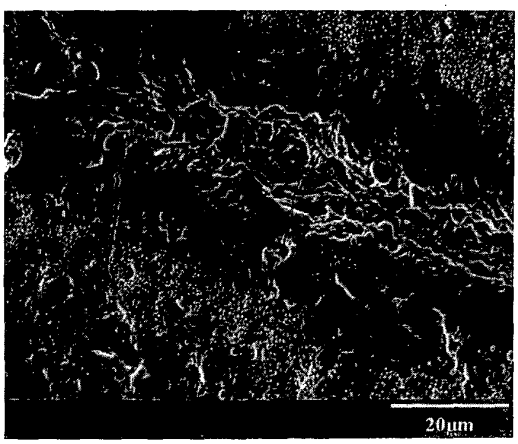

Figure 11. Conductive flashover path of an MBT insulator that shows thermal cracking and melting of the insulator.

terial. A closer image of the discharge path is shown in Figure 10. The relative bright contrast of the surrounding oxide to the same oxide in the channel is due to electrode deposition at the edges of the path. The smooth, rounded channel features, large cracks along the discharge path, and the faint white ribbon in the center of the discharge channel indicates that large temperature variations leading to melting, cracking, and disassociation of the insulator material were present. The milky white ribbon is believed to a Ti rich phase and also the conduction path that radiates upon nominal voltage applications after failure. The melting of the insulator is even more prevalent in MBT samples as shown in Figure 11. EDS chemical analysis at the center of the jagged ribbon showed higher peaks for Ba and Ti than EDS performed on the bare insulator surface, indicating again that the ribbon is composed of Ti and Ba rich phases. The jagged nature and localized small gaps in the melted insulator explains why the electrode gap can withstand small voltages after failure, but upon the application of a few hundred volts, radiates from resistive heating. The resistance of the formed conductive channel was found to be greater than 10 MΩ at a 1 V bias which explains why the gap can hold off small voltages after failure.

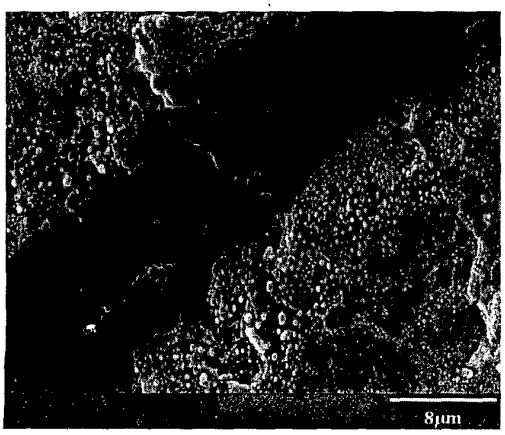

Figure 10. Conductive flashover path of a TiO_2 insulator that illustrates the thermal cracking and melting of the insulator.

To determine whether this observed failure was due to high dielectric constant of the insulator, insulator thermal properties, or thin film electrodes, a few samples of PTFE, NaCl, and fused quartz were prepared with 1.5 mm electrode gaps in the same manner as the other insulators and subjected to dc surface flashover experiments.

Upon flashover the PTFE melted predominantly at the cathode and partially at the anode, causing effective switch failure either through vaporization and widening of the gap by or coating the electrode with molten insulator. The NaCl samples failed catastrophically by thermo-mechanically cracking and locally melting at the anode and cathode. Although both of these insulators failed, they did not fail as severely as did the TiO_2 and MBT samples. The fused quartz samples failed in the same manner as the MBT and TiO_2 samples, but after 15 to 30 flashovers. These results indicate that the thermal properties of the insulator are primarily responsible for the observed failure, but a dielectric constant effect is also observed as noted by the fact that the fused quartz has a lower thermal conductivity and melting temperature than MBT or TiO_2, but did not fail until after 10 to 25 more flashovers. MBT, TiO_2, Al_2O_3, NaCl, PTFE, and fused quartz samples were subjected to continuous dc surface flashover with 45° angled solid stainless steel electrodes clamped to the surface of the insulator to determine if the observed failure was independent of thin electrodes. None of the samples failed except for PTFE which melted at the anode and cathode. All the insulator surfaces exhibited very limited electrode deposition and bulk heating, even after thousands of consecutive multiple channel breakdowns.

The observation that all of the insulators did not fail even after thousands of discharges with solid electrodes, and that the solid electrodes did not deposit metal in the gap, indicates that the failure mechanism is dependent on the presence of metal species in the gap. Al_2O_3, which has a lower dielectric constant, higher thermal conductivity, and higher melting temperature than the other insulators, did not exhibit this failure mechanism and indicates that the thermal properties of the insulator are also key to the failure. The observation of fused quartz failing similarly to the titanates, but only after many flashovers might be explained by Beverly's observations of increased UV radiation from flashovers across titanate ceramics which lead to higher radiative heating across the titanate surface [24]. Also, the observation of the flashover path traversing the gap closer to the surface for higher dielectric constant insulators would lead to an enhanced heat transfer to the surface. Previous studies and calculations have shown that the total radiated energy is 80% of the electrically measured energy dissipated in the gap [27]. Latent heat calculations of the channel formation indicates that enough electrical energy is transferred upon 10 to 15 flashovers to form the observed melted channel. However, this energy does not all manifest as heat in the gap through radiative heat transfer, it is also transferred into electrode heating and radiation directed away from the surface. The jagged nature of the path indicates that the failure channel was indeed formed where a large flashover path was and indicates the channel was formed from some mode of heat transfer from the flashover plasma. In accordance with these results it was noted that the failure mechanism is due to a combination of insulator dielectric constant and thermal properties, and the presence of metallic species in the gap region during flashover. Elucidation of the exact mechanism of this channel formation is currently being studied.

3.2 TRIGGERED SURFACE FLASHOVER

Typical current and voltage signals obtained upon triggered flashover across the surface of Al_2O_3 are shown in Figure 12. Two distinct current waveforms are observed in the signal. The first waveform is attributed to the high voltage pulse leading to a flashover between the trigger electrode and the cathode which creates a current flow from the trigger to the cathode and corresponding slight decrease in the gap potential. The second waveform is attributed the surface flashover between the switch anode and cathode which creates a current flow from the anode to the cathode and the total decay of the gap potential. The second current waveform is similar in form and magnitude to the one observed during dc flashover and shows the corresponding gap potential decay as shown in the voltage signal. The delay between the trigger voltage and the total anode to cathode switch flashover was observed to range from 500 to 2200 ns. Figure 13 shows typical current and voltage signals obtained from triggered flashover across an MBT insulator. The current waveform from the trigger flashover is seen to overlap with the current waveform from the anode to cathode flashover, while the voltage signal rapidly decreases to zero as is observed upon dc surface flashover. This type of triggered flashover was always observed across MBT and was usually seen across TiO_2. However, approximately 1 in 10 flashovers across TiO_2 demonstrated a delay of a 100 to 200 ns between the trigger voltage and the anode to cathode current.

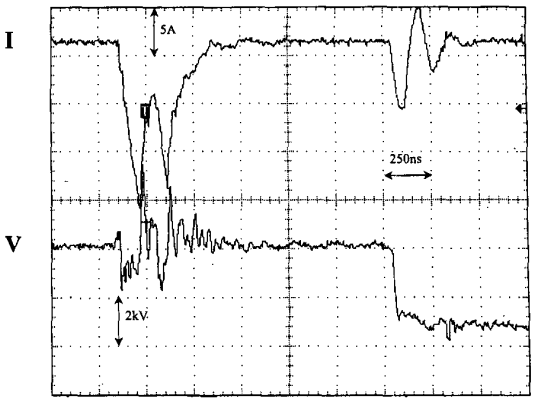

Figure 12. Typical current and voltage signals during a triggered flashover across an Al_2O_3 insulator.

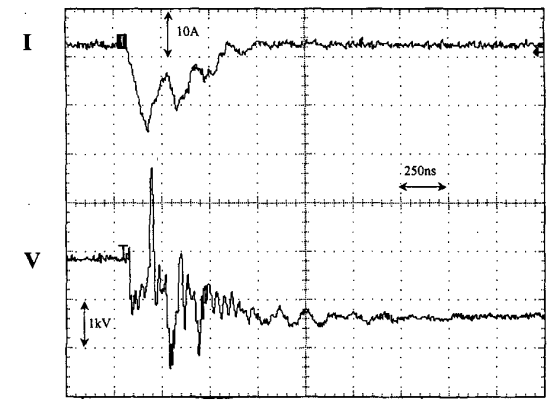

Figure 13. Typical current and voltage signals during a triggered flashover across a MBT insulator.

The delay time and jitter of the first current peak with respect to the trigger voltage is given in Table 5. In all cases, the delay time was found to be approximately 20 ns

Table 5. Triggered flashover characteristics with varying trigger voltage.

	+2kV Trigger		+1kV Trigger	
Insulator	Delay time (ns)	Jitter (ns)	Delay time (ns)	Jitter (ns)
Al_2O_3	20.3	5.9	21.8	7.6
TiO_2	22.3	4.3	20.0	6.0
MBT	25.0	4.9	22.3	5.6

Table 6. Observed lifetime values for insulators during triggered flashover.

	Screen Printed Electrodes			Sputtered Electrodes		
Insulator	Air	Vacuum	SF2	Air	Vacuum	SF2
Al_2O_3	> 200	> 200	> 200	41 ± 11	< 3	< 3
TiO_2	> 200	< 3	< 3	41 ± 8	< 3	< 3
MBT	> 200	< 3	< 3	34 ± 8	< 3	< 3

with a corresponding jitter of 6 ns, and did not significantly vary with the magnitude of the applied trigger voltage. However, this jitter value might not correspond to the actual switch jitter, as these values represent the initial current transfer and do not necessarily represent the total switch delay time and jitter. One realistic reason for the unsuspected large delay times and jitter is the trigger electrode positioning [5]. The single wire trigger approach was used as it was the easiest way to electrically trigger the proposed device, however it leads to non-uniform field distributions in the electrode gap and initially triggers only a small region of the gap. A thin long trigger wire traversing the length of the cathode just below the surface at 0.25 mm would likely improve the switch performance drastically [28], but it is not reasonable for use in the DWA.

The triggered flashover lifetimes in air for all three insulators with both screen printed and sputtered electrodes were much higher than dc values as shown in Table 6. The sputtered electrode lifetimes in air increased nearly tenfold, and all the screen printed electrode lifetimes in air were greater than 200 flashovers. The lifetimes in vacuum and SF-2 were still limited to only one or two flashovers for TiO_2 and MBT samples due to the formation of conductive channels during catastrophic multiple channel flashover. All lifetimes shown in Table 6 are for a triggered gap with a dc bias of less than 50% of the self flashover value. With an increase of the dc bias to only 55 to 60%, the lifetimes in air decreased to dc flashover values for both TiO_2 and MBT.

4 CONCLUSIONS

dC surface flashover and triggered flashover experiments were conducted at 1atm, 0.13 Pa, and in an insulating fluid with thin film electrodes on insulators with varying dielectric constant. dc flashover voltages were negatively related to the dielectric constant of the insulator and were found to have a linear dependence with electrode separation distance for 15 μm screen printed electrodes and a square root dependence for 0.25 μm sputtered electrodes. Electrostatic field modeling of localized electrode polarization was used to explain the decrease in flashover voltage with increased insulator dielectric constant. A variation in the flashover path trajectory was observed and was related to the attraction of the initial charge carriers to the surface due to increased polarization from insulators with higher dielectric constants. Triggered flashover current delay times were observed to be approximately 20 ns with a corresponding jitter of about 6 ns. Short lifetimes were found for the thin film electrode/insulator combinations except for carefully controlled, triggered switching on gaps dc biased to 50% self flashover utilizing screen printed electrodes in an air atmosphere. Short lifetimes were attributed to multiple channel flashover leading to the formation of a conductive channel across the electrode gap. Although the exact failure mechanism is not fully understood, it has been shown to be due to a combination of insulator thermal and dielectric properties and the presence of metallic species in the gap region during flashover.

REFERENCES

[1] H. C. Miller, "Surface Flashover of Insulators", IEEE Trans. EI, Vol. 24, pp. 765–786, 1989.

[2] R. Latham, *High Voltage Vacuum Insulation*. Academic Press, San Diego, CA 1995.

[3] Neuber, M. Butcher, L. L. Hatfield, and H. Krompholz, "Electric Current in DC Surface Flashover in Vacuum", J. Appl. Phys., Vol. 85, pp. 3084–3091, 1999.

[4] Neuber, M. Butcher, H. Krompholz, L. L. Hatfield, and M. Kristiansen, "The Role of Outgassing in Surface Flashover Under Vacuum", 12th IEEE Int. Pulsed Power Conference, Monterey, CA, 1999.

[5] G. Schaefer, M. Kristiansen, and A. Guenther, *Gas Discharge Closing Switches*. Plenum Press, New York, 1990.

[6] M. J. Kofoid, "Effect of Metal-Dielectric junction Phenomena on High-Voltage Breakdown Over Insulators in Vacuum", AIEE Transactions, Vol. 6, pp. 999–1004, 1960.

[7] T. S. Sudarshan, "Electrode Architecture Related to Surface Flashover of Solid Dielectrics in Vacuum", IEEE Trans. DEI, Vol. 4, pp. 374–381, 1997.

[8] G. Caporaso, S. Sampayan, H. Kirbie, "Dielectric-wall Linear Accelerator With a High Voltage Fast Rise Time Switch that Includes a Pair of Electrodes Between which are Laminated Alternating Layers of Isolated Conductors and Insulators", US Patent 5821705, 1996.

[9] S. Sampayan, G. Caporaso, H. Kirbie, "Enhanced Dielectric-wall Linear Accelerator", US Patent 5811944, 1998.

[10] S. Sampayan, G. Caporaso, B. Carder, Y. Chen, C. Holmes, E. Lauer, D. Trimble, J. Elizondo, M. Krogh, B. Rosenblum, C. Eichenberger, J. Fockler, "High Gradient Insulator Technology for the Dielectric Wall Accelerator", Proc. Particle Accelerator Conference, 1995, p. 1269.

[11] S. Sampayan, G. Caporaso, B. Carder, M. Norton, D. Trimble, J. Elizondo, "Optically induced surface flashover switching for the dielectric wall accelerator", Proc. Particle Accelerator Conference, p. 2123, 1995.

[12] R. A. Anderson and J. P. Brainard, "Mechanism of Pulsed Surface Flashover Involving Electron-Stimulated Desorption", J. Appl. Phys., Vol. 51, pp. 1414–1421, 1980.

[13] M. H. Lean and D. S. Bloomberg, "Nonlinear Boundary Element Method for Two-Dimensional Fields", J. Appl. Phys., Vol. 55, pp. 2195–2197, 1984.

[14] J. Rikabi, "A Convergence Index for Field Solutions in Nonlinear Media", Int. J. Num. Modeling, Vol. 4, pp. 75–80, 1991.

[15] Smith, G. Lauer, and M. Levine, "Tests of a Dielectric-Vacuum Surface Flashover Switch", in Proc. 15th Power Modulator Symp., p. 160, 1982.

[16] G. Blaise, "The Space Charge Physics and the Breakdown Process", Annual Report of Conference on Electrical Insulation and Dielectric Phenomena, pp. 98–103, 1993.

[17] H. M. von Bergmann, "Triggered Multichannel Surface Spark Gaps", J. Phys. E: Sci. Instrum., vol. 15, p. 243, 1982.

[18] T. Suzuki, "Flashover Voltage Over Ceramics in High Vacuum", Japan J. Appl. Phys., Vol. 13, pp. 1541–1546, 1974.

[19] Watson, A. L. Donaldson, K. Ikuta, M. Kristiansen, "Mechanism of Electrode Surface Damage and Material Removal in High Current Discharges", IEEE Trans. on Magnetics, Vol. 22, p. 1448, 1986.

[20] R. H. Fowler and L. Nordheim, "Electron Emission in Intense Electric Fields", Proc. R. Soc. Lond. A, vol. 119, pp. 173–181, 1928.

[21] T. Asokan and T. S. Sudarshan, "Dependence on the Surface Flashover Properties of Alumina on the Polishing Abrasive Parameters", IEEE Trans. EI, Vol. 28, pp. 535–544, 1993.

[22] Mitra, T. Asokan, T. S. Sudarshan, "Surface flashover performance of chemically etched polycrystalline alumina", Annual Report of Conference on Electrical Insulation and Dielectric Phenomena, pp. 318–323, 1993.

[23] T. S. Sudarshan and C. R. Li, "Dielectric Surface Flashover in Vacuum: Experimental Design Issues", IEEE Trans. DEI, Vol. 4, pp. 657–662, 1997.

[24] R. E. Beverly, "Electrical, Gasdynamic, and Radiative Properties of Planar Surface Discharges", J. Appl. Phys., Vol. 60, pp. 104–124, 1986.

[25] A. L. Donaldson, M. O. Hagler, M. Kristiansen, G. Jackson, and L. Hatfield, "Electrode Erosion Phenomenon in a High-Energy Pulsed Discharge", IEEE Trans. On Plasma Science, Vol. PS-12, pp. 28–38, 1984.

[26] H. Moscicka-Grzesiak and Z. Banaszak, "Surface Dielectric's Properties of Cu-Evaporated Alumina Insulators in Vacuum and Air", IEEE Proc. 3rd Int. Conf. On Properties and Applications of Dielectric Materials, Vol. 1, pp. 627–630, 1991.

[27] P. N. Dashuk, A. K. Zinchenko, M. D. Yarysheva, "Erosion of dielectrics in the switching of high-pulsed currents by a grazing discharge", Sov. Phys. Tech. Phys., Vol. 26, pp. 196–201, 1981.

[28] R. Curry, D. Johnson, M. Kristiansen, L. Hatfield, and A. H. Guenther, "Triggering of Surface Discharge Switches", IEEE Proc. 4th IEEE Pulsed Power Conf., Vol. 1, pp. 174–177, 1983.

[29] D. R. Lide, *CRC Handbook of Chemistry and Physics 74th Edition*. CRC Press, Ann Arbor, 1993.

[30] J. D. Cox, D. D. Wagman, V. A. Medvedev, *CODATA Key Values for Thermodynamics*. Hemisphere Publishing Corp., New York, 1984.

Manuscript received on 9 October 2000, in final form 23 November 2001.

Currently at 577 Evans Hall, University of California-Berkeley, Berkeley, CA 94720, USA.